

# Application of a Modular Particle-Continuum Method to Hypersonic Propulsive Deceleration

Timothy R. Deschenes\*, Hicham Alkandry† and Iain D. Boyd‡

*Department of Aerospace Engineering, University of Michigan, Ann Arbor, MI, 48109*

A modular particle-continuum (MPC) method is used to quantify the effect of continuum breakdown on aerodynamic predictions of Mach 12 hypersonic flow over a Mars entry aeroshell with a single-nozzle, sonic propulsive decelerator (PD). The MPC method loosely couples an existing direct simulation Monte Carlo (DSMC) code to a Navier-Stokes solver (CFD). Previous studies have shown that the MPC method can maintain the physical accuracy of DSMC in regions where the Navier-Stokes equations break down, while achieving the computational efficiency of CFD in regions that are considered fully continuum. Due to the very high number density within the jet core, application of the DSMC method across the entire flow field is computationally expensive, and unnecessary. Comparison of predictions made by full CFD and the MPC method are performed at low and high thrust conditions. It is found that the jet induces an increase in the size of the rarefied region compared to the jet off configuration. Despite the additional mass added by the jet at high thrust, the degree of rarefaction is found to increase due to the intensification in flow gradients in the jet expansion region. In addition, it is found that the MPC results predict a larger recirculation region in the jet-shock layer interaction region compared to continuum predictions. The continuum aerodynamic drag coefficients are under predicted by 6% at low thrust configuration and over predicted by a factor of 2.7 at the high thrust condition. However, total axial force predictions made by continuum and hybrid methods are in very good agreement at both thrust conditions.

## Nomenclature

$A$	Area [m <sup>2</sup> ]
$Br$	Breakdown parameter
$Kn_{GL}$	Gradient-length Knudsen number
$D$	Drag [N]
$P$	Pressure [Pa]
$Q$	Macroscopic flow quantity
$T$	Thrust [N]
$T_{ROT}$	Rotational temperature [K]
$T_{TRA}$	Translational temperature [K]
$ V $	Bulk speed [m/s]
$U_{\infty}$	Free stream velocity [m/s]
$\lambda$	Mean free path [m]
$\rho_{\infty}$	Free stream density [kg/m <sup>3</sup> ]
$\tau$	Shear stress [Pa]

\*Research Fellow, AIAA Member. Email: thytimo@umich.edu.

†Graduate Student, AIAA Student Member. Email: halkandr@umich.edu.

‡James E. Knott Professor of Engineering, Fellow AIAA. Email: iainboyd@umich.edu.

## I. Introduction

Alternative entry, descent, and landing (EDL) technologies are needed for future high-mass Mars entry systems due to mass and size limitations of the current conventional aerodynamic decelerators. One of these technologies may be propulsive decelerator (PD) jets, which can be used to slow the vehicle during atmospheric descent by directing engine thrust into the oncoming free stream. Several different EDL architectures for human-scale Mars missions are currently being considered,<sup>1</sup> which include an all-propulsive design with PD jets firing into an incoming hypersonic free stream. The use of these jets, however, involves complex flow interactions that are still not well understood. Continuum methods, mainly Computational Fluid Dynamics (CFD), are currently being used as tools to investigate these interactions. However, due to relatively low densities associated with many hypersonic flows, the continuum approximation may not hold for some regions in the flow field and the application of these methods over the entire flow field may be inappropriate. Previous studies<sup>2-4</sup> of the effect of continuum breakdown for hypersonic flows have been performed, but were limited to flows that did not contain any jet interactions. Typically, a fully kinetic method, such as the direct simulation Monte Carlo (DSMC) method, is used to examine rarefied flows. However, due to the very high density in the core of the PD jet, it is computationally infeasible to apply DSMC over the entire flow field. Instead, a hybrid method<sup>5,6</sup> can be used that applies the DSMC method only in regions of the flow that are rarefied, uses a continuum method in regions of the flow where the Navier-Stokes equations are valid, and couples the two in a physically consistent manner.

This study compares the flow field, surface, and aerodynamic properties of a Mars entry aeroshell with a single-nozzle sonic PD jet using continuum and hybrid particle-continuum computational methods in order to understand the effect of continuum breakdown on the flow field quantities, surface properties, and integrated aerodynamics of the aeroshell. Section II outlines the background of the study including the definition of geometry and flow conditions and a description of the continuum and hybrid methods. Section III compares full CFD and MPC predictions of macroscopic field quantities, surface properties, and integrated aerodynamic coefficients. Finally, conclusions drawn from these simulations are described in Sec. IV.

## II. Background

### Geometry and Flow Conditions

A scaled Mars Science Laboratory (MSL) aeroshell is used in this study. The diameter of the aeroshell is 10 mm, which is equivalent to approximately 0.22% the size of the MSL capsule. The PD jet is located at the center of the fore-body. The PD nozzle consists of a converging section, with a nozzle-exit diameter of 0.5 mm. The gas used is diatomic nitrogen and the aeroshell surface is modeled as an isothermal wall with a temperature of 300 K. The Ashkenas and Sherman<sup>7</sup> boundary conditions are used in this study to describe the free stream conditions and are implemented in the continuum and hybrid codes. These flow conditions and geometric representation correspond to hypersonic free-jet experiments that are currently being conducted at the University of Virginia to also study the interactions between the PD jets and a hypersonic free stream.<sup>8-10</sup> As a result, a set of reference free stream conditions is obtained using isentropic relations for a reference free stream at a Mach number of 12, a stagnation pressure of  $1.8 \times 10^5$  Pa, and a stagnation temperature of 300 K, which are used to compute non-dimensional quantities, such as the drag coefficient. The boundary conditions for the PD jet are computed such that sonic conditions ( $M_{jet} = 1.0$ ) are obtained at the nozzle-exit. These conditions are non-dimensionalized using the thrust coefficient,<sup>11</sup> shown in Eq. 1, which is the ratio of the thrust produced by the nozzle to the product of the reference free stream dynamic pressure and the aeroshell frontal area.

$$C_T = \frac{T}{\frac{1}{2}\rho_\infty U_\infty A_{shell}} \quad (1)$$

Table 1 presents the total pressure ratios for the thrust coefficient of the previous study performed by Alkandry et al.<sup>12</sup> In this study, due to the complexity of the flow, the MPC method is applied to a low thrust coefficient ( $C_T = 0.5$ ) and a high thrust coefficient ( $C_T = 2.0$ ) and results are compared to continuum predictions to quantify the effect of continuum breakdown.

Figure 1 presents Mach number contours and highlights the relevant flow features for the 0.5 thrust coefficient conditions predicted by the continuum method. The PD jet expands from sonic conditions at the nozzle-exit to higher, supersonic Mach numbers. The flow then decelerates from supersonic to subsonic

Table 1: PD jet conditions ( $P_{0,\text{main}} = 1.8 \times 10^5$  Pa)

$C_T$	0.5	1.0	1.5	2.0	2.5
$P_{0,\text{jet}}/P_{0,\text{main}}$	0.11	0.22	0.33	0.44	0.55

conditions through a jet shock and then from subsonic to zero velocity at a stagnation point detached from the surface of the aeroshell. The free stream also decelerates from hypersonic to subsonic velocities through a bow shock and then to zero velocity at the same stagnation point. In the interface region (region between the bow and jet shocks where the two streams mix), the total pressures for the two streams are equal as they both flow outward between the two shocks with subsequent re-acceleration to supersonic velocities. The figure also shows a region of separated flow between the PD jet boundary, the surface of the model and the mixed outflow, with a reattachment point near the shoulder of the aeroshell.

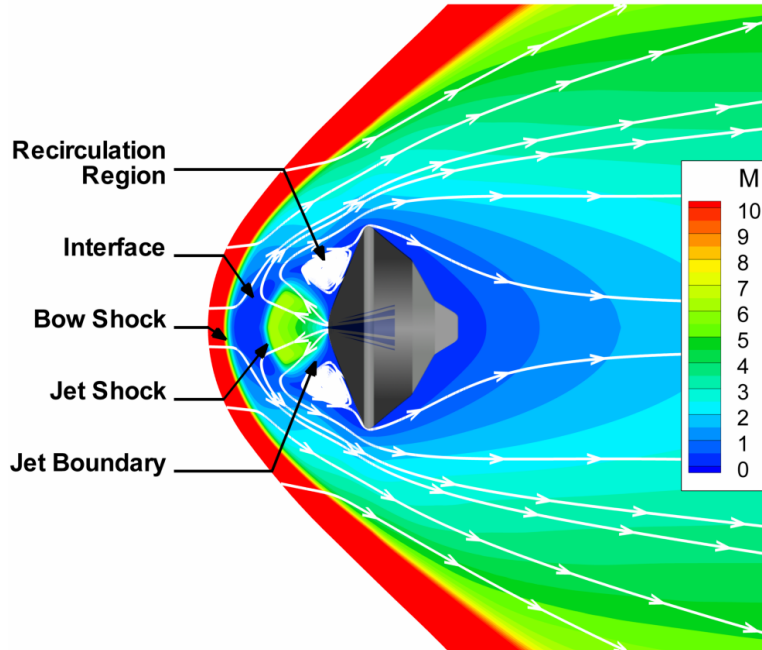


Figure 1: PD jet flow field features for  $C_T = 0.5$

## Continuum Method

The continuum code, LeMANS, which is used in this study was developed at the University of Michigan for simulating hypersonic, reacting flows.<sup>13-15</sup> This general purpose, three-dimensional, parallel code solves the laminar Navier-Stokes equations on unstructured computational grids including thermo-chemical nonequilibrium effects with second-order accuracy. The flow is modeled assuming that the continuum approximation is valid. In this work, it is assumed that the translational and rotational energy modes of all species can be described by two different temperatures  $T_{\text{TRA}}$  and  $T_{\text{ROT}}$ ,<sup>4</sup> respectively, while the vibrational energy mode and electronic energy of all species are described as being frozen throughout the flow field. In LeMANS, the mixture transport properties can be computed using several options. In this study, the variable hard sphere (VHS)<sup>16</sup> model is used to ensure that the transport properties are the same in both the continuum and hybrid methods. The finite-volume method applied to unstructured grids is used to solve the set of partial differential equations. A modified version of the Steger-Warming flux vector splitting scheme is used to discretize the inviscid fluxes across cell faces, which is less dissipative and produces better results in boundary layers compared to the original scheme. The viscous terms are computed using cell-centered and nodal values. Time integration is performed using either a point implicit or a line implicit method. LeMANS is parallelized using domain decomposition.

## Continuum Breakdown

For many cases, the global Knudsen number can be used to characterize the flow as continuum or rarefied. However, some flow features, such as shocks and shear layers, may have length scales that are sufficiently small compared to the mean free path that the continuum assumption breaks down in these regions while the rest of the flow is well within the continuum limit. One way of predicting the continuum breakdown in a mixed rarefied-continuum flow is with the gradient-length Knudsen number, shown in Eq. 2, where  $\lambda$  is the local mean free path and  $Q$  is some local flow quantity of interest such as density, flow speed, or temperature. It has been found<sup>17, 18</sup> that when the maximum of the gradient-length Knudsen number, shown in Eq. 3, exceeds 0.05, the difference between CFD and DSMC predictions exceed 5%. However, continuum methods may be applied to the entire flow field if the rarefied portion has a very small effect on the outputs of interest. For example, the low density wake region behind hypersonic, blunt bodies often display non-continuum effects. For many cases, aerodynamic coefficients are insensitive to the surface quantities in this region since the contribution to the total net force is very small. Previous studies of non-continuum effects<sup>3, 4, 19</sup> on flow fields and surface properties have shown continuum models can provide sufficiently accurate prediction of aerodynamics for flows with global Knudsen number less than 0.01. This is because most of the rarefied regions are isolated to the near wake region, and bow shock and prediction of fore-body surface quantities are insensitive to both of these regions. For the flow conditions of interest in this study, the global Knudsen number based on reference flow quantities is 0.006 which suggests that the overall flow should lie in the near-continuum regime.

$$Kn_{GL-Q} = \lambda \left| \frac{\nabla Q}{Q} \right| \quad (2)$$

$$Kn_{GL-MAX} = \max (Kn_{GL-\rho}, Kn_{GL-T_{TRA}}, Kn_{GL-T_{ROT}}, Kn_{GL-|V|}) \quad (3)$$

Figure 2 shows contours of the  $Kn_{GL-MAX}$  calculated from the continuum prediction for hypersonic flow over an aeroshell with a propulsive decelerator at thrust coefficients of  $C_T = 0.5$  (top) and  $C_T = 2.0$  (bottom). Similar to previous studies,<sup>3, 4, 19, 20</sup> when the PD jet is not used, the rarefied portion of the flow is isolated to the detached bow shock and low density, near wake region. However, when the PD jet is used, the gradient-length Knudsen number is higher than the breakdown value of 0.05 over most of the fore-body. Despite the PD jet adding additional mass to the flow field, it also induces large gradients along the entire fore-body of the aeroshell. Typically, the effect of continuum breakdown is examined with a rarefied simulation technique, such as the DSMC method.<sup>2, 21</sup> However, the very small collision length- and time-scales within the interior of the PD jet significantly increases the computational cost of applying the DSMC method across the entire flow. For example, Fig. 3 shows the variation in collision length scales about the aeroshell with a thrust coefficient of  $C_T = 0.5$  (top) and  $C_T = 2.0$  (bottom). The variation in collision length scales between the high density jet and low density, near wake region exceeds 6 orders of magnitude and the computational expense required to resolve the jet core by the DSMC method is prohibitively expensive.

## Modular Particle-Continuum (MPC) Method

Typically, the DSMC method is applied to flows that exhibit rarefied effects. However, the region of the flow within the converging nozzle and the PD jet core has a much higher density than the rest of the flow field. The high collisionality experienced in the jet region is exactly where the Navier-Stokes are valid and CFD can be used to accurately *and* efficiently simulate the flow. Therefore, this work uses a hybrid approach with the Modular Particle-Continuum (MPC) method to examine the effect of continuum breakdown on the prediction of flow field, surface, and aerodynamic properties of aeroshells with propulsive decelerators.

The MPC method was developed to be capable of simulating one-dimensional shock waves<sup>22</sup> and both axisymmetric and two-dimensional steady state hypersonic flows.<sup>5, 6</sup> It uses the LeMANS<sup>13, 14</sup> code, described in a preceding subsection for the continuum regions, while using the DSMC code, MONACO,<sup>23</sup> to simulate the rarefied regions. The interface region is determined by a local gradient-based Knudsen number as denoted by Eq. 3.<sup>17, 18</sup> This study uses a cutoff parameter,  $Br_{cutoff}$ , of 0.1 such that DSMC is used in regions where  $Kn_{GL-MAX} > Br_{cutoff}$  and CFD is used elsewhere. This is higher than the cutoff parameter proposed by Boyd et al.<sup>17, 18</sup> which was developed through detailed comparison of full DSMC and full continuum simulation results. However, it has been shown<sup>20, 24</sup> that the continuum module can maintain a high level of physical accuracy up to higher local Knudsen numbers with the improved boundary conditions provided by the DSMC method in a hybrid methodology. Previous studies<sup>6, 20, 24, 25</sup> have shown that MPC predictions are

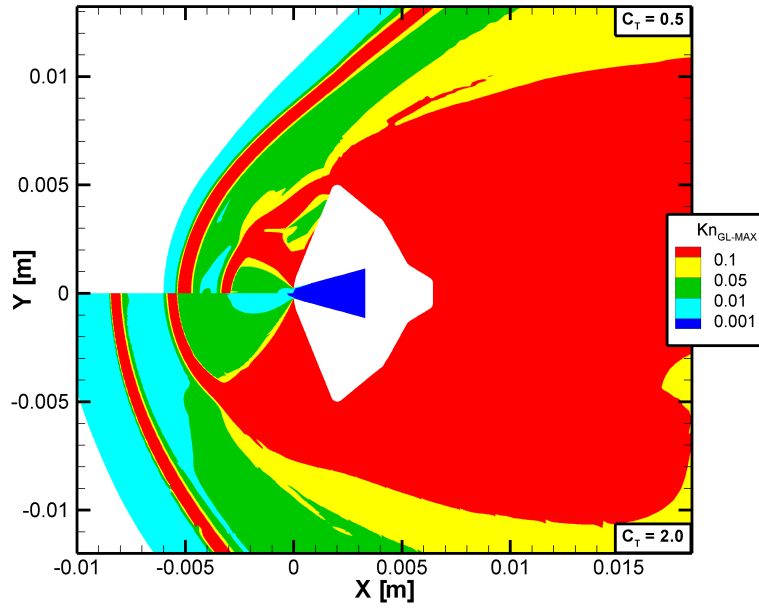


Figure 2: Maximum gradient-length Knudsen number for hypersonic flow over the aeroshell at thrust coefficients of  $C_T = 0.5$  (top) and  $C_T = 2.0$  (bottom)

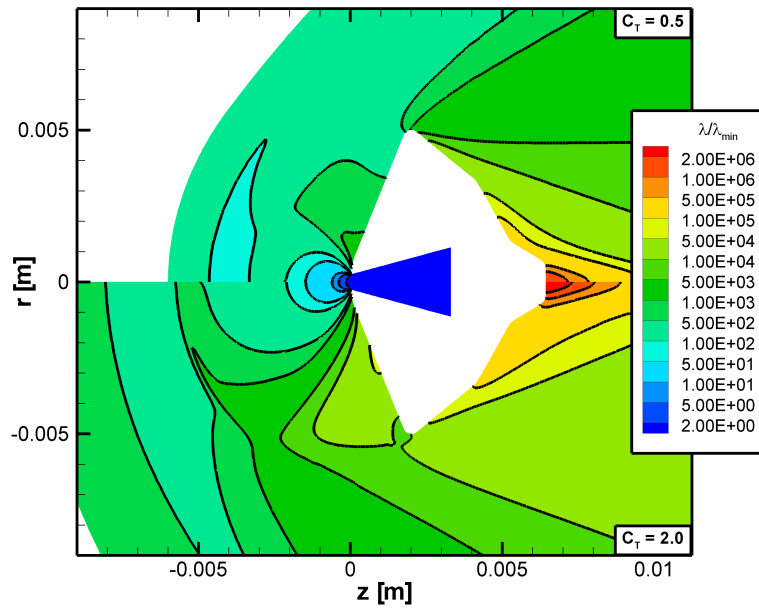


Figure 3: Variation in collision length- and time-scales around the aeroshell at thrust coefficients of  $C_T = 0.5$  (top) and  $C_T = 2.0$  (bottom)

in excellent agreement with full DSMC results for flow field quantities, surface properties, and probability density functions.

MONACO<sup>26</sup> is a general, cell-based implementation of the DSMC method capable of simulating rotational<sup>27</sup> and/or vibrational<sup>28</sup> nonequilibrium flow with an arbitrary number of species with finite rate chemistry. For the results used in this paper, the variable hard sphere (VHS) collision model is used which reproduces the macroscopic viscosity model used within the continuum module.

Each code (continuum and rarefied) is allowed to maintain its own data structure within the MPC method and the two are loosely coupled using a state-based coupling procedure. The density, velocity, and temperatures are tracked in the DSMC boundary cells using a relaxation average<sup>29</sup> that weights each iteration a small fraction compared to the average based on all previous time-steps, which reduces the scatter experienced in the DSMC method.<sup>22</sup>

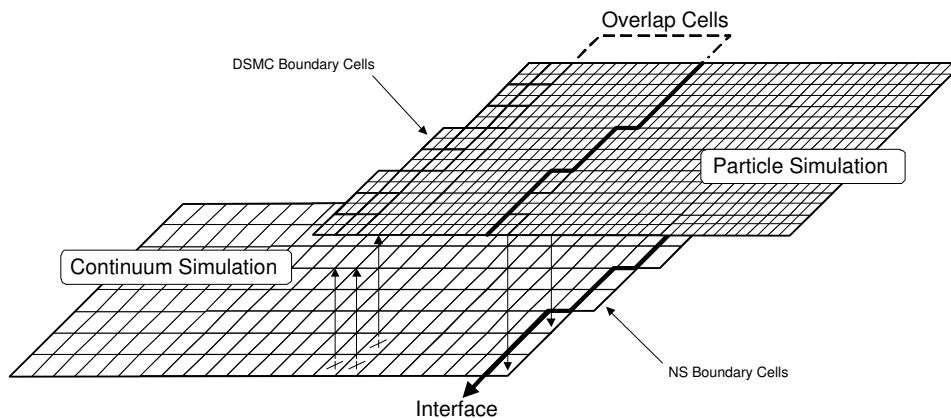


Figure 4: Schematic of the modular mesh structure and coupling between solvers at an interface location

An overlap region is used to ensure that the CFD-DSMC boundaries are positioned in continuum regions.<sup>5</sup> An MPC simulation begins with the full CFD solution and applies the breakdown parameter to estimate the regions of flow that exhibit rarefied effects. The DSMC region is then extended and the breakdown parameter is periodically applied to the current flow solution to ensure that the entire rarefied portion of the flow is simulated with DSMC. After the interface locations have stopped moving and the flow has reached steady-state, the overlap regions are removed, and DSMC sampling procedures are performed to reduce the statistical scatter while CFD is iterated to reduce the residual. Figure 4 shows a schematic of computational meshes and state-based coupling procedures near an interface location during the unsteady portion of an MPC simulation.

### III. Results

Simulations of Mach 12 flow over an aeroshell at two thrust coefficients are performed with the MPC method and compared to the corresponding continuum prediction. Figure 5 shows the initial and final interface locations for both thrust conditions. In general, the final interface location is nearly the same as the initial interface location, except in the recirculation region at the low thrust coefficient. Here, the hybrid method adaptively reduces the size of the continuum region as the flow progresses from the initial continuum prediction to the final MPC prediction. Interface locations and flow field quantities are compared at different simulation intervals to ensure that the flow reached steady state before locking the interfaces and sampling the DSMC region to reduce the statistical scatter in the outputs of interest. The same mesh density is used for both continuum and hybrid simulations and consists of approximately  $10^5$  computational cells. The DSMC portion of the hybrid domain consists of approximately  $28 \times 10^6$  simulation particles and requires a total CPU time of a factor of 2.7 times larger than the corresponding continuum CPU time. More details of the continuum simulation requirements can be found in Ref. 12.

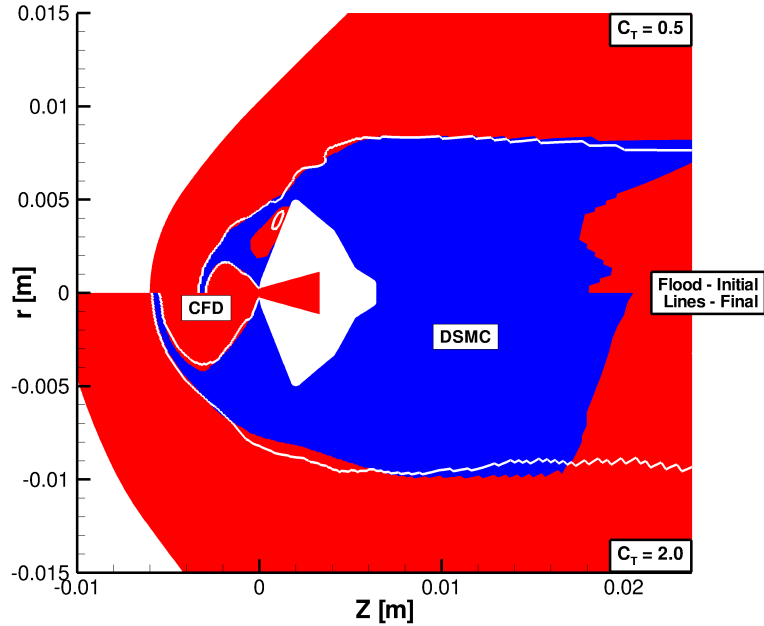


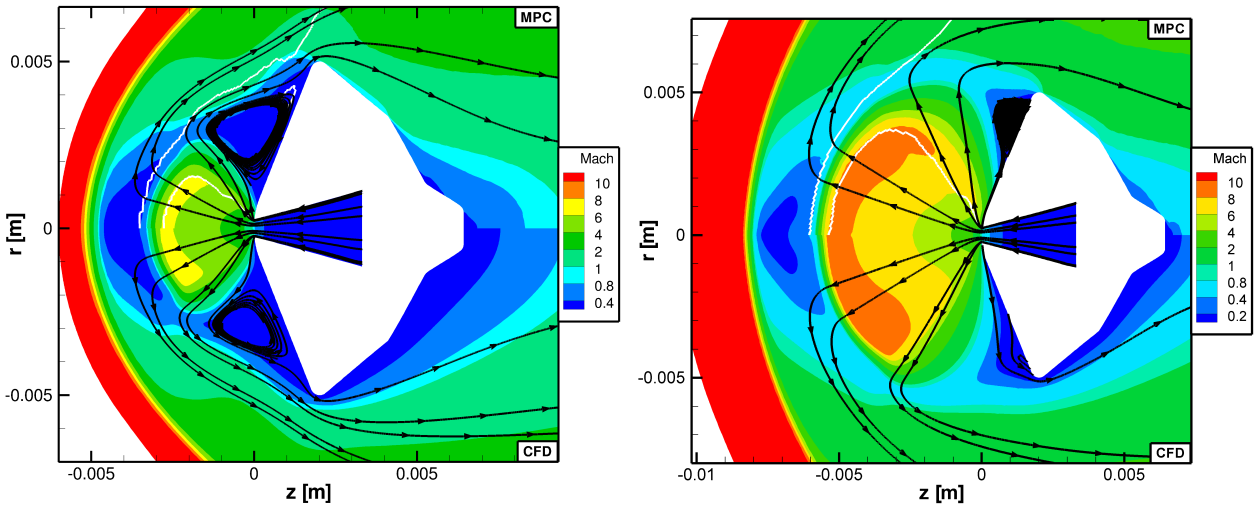
Figure 5: Initial and final DSMC-CFD interface location used by the MPC method for Mach 12 flow over an aeroshell at thrust coefficients of  $C_T = 0.5$  (top) and  $C_T = 2.0$  (bottom)

### Flow Field Properties

Figure 6 compares Mach number contours and stream traces based on the bulk velocity predicted by the MPC method (top) and full CFD (bottom) at both thrust conditions. For each streamline, the initialization points are selected in identical locations within MPC and CFD predictions so any difference in stream trace locations are due to differences in the flow field predictions. In general, Mach number contours predicted by each method are in good agreement in the PD jet-shock layer interaction region at the low thrust condition. However, the MPC method predicts a larger recirculation zone in the fore-body region. One factor contributing to the increased size of the recirculation zone is the reduction in momentum transfer to the surface of the body, which is evident in the surface shear stress prediction shown in the proceeding subsection. In the expansion around the shoulder and near wake region, the MPC method predicts a higher Mach number nearer the surface. This is due to a combination of two effects. First, the DSMC method, which is used by the MPC method along the surface, allows a velocity slip so that the velocity is higher near the surface in the MPC results. Secondly, due to the low free stream temperatures associated with the expansion tunnel used, the aeroshell heats the surrounding fluid and the temperature of the fluid near the body is lower in the MPC results due to temperature jump. This reduces the local speed of sound near the wall. Similar trends are seen in the expansion around the shoulder and near wake region at the high thrust coefficient. However, now the differences in prediction of the fore-body and recirculation are more pronounced. The MPC method predicts a recirculation region that is significantly larger than that predicted by full CFD. In addition, the increase in strength of the expansion near the edge of the PD jet predicted by the MPC method is evident in the widening of distance between stream lines as they are turned by the expansion of the jet.

Figure 7 shows the prediction of flow near the strong expansion in the PD jet and surface interaction region made by the MPC method (top) and full CFD (bottom) at each thrust coefficient. The effect of velocity slip is evident at both thrust conditions as the MPC results predict a higher speed near the wall which reduces the size of the boundary layer and increases the turning angle of the flow. Again, the disagreement between MPC and continuum predictions increases as the thrust coefficient increases despite the higher density (due to higher mass flux from the jet).

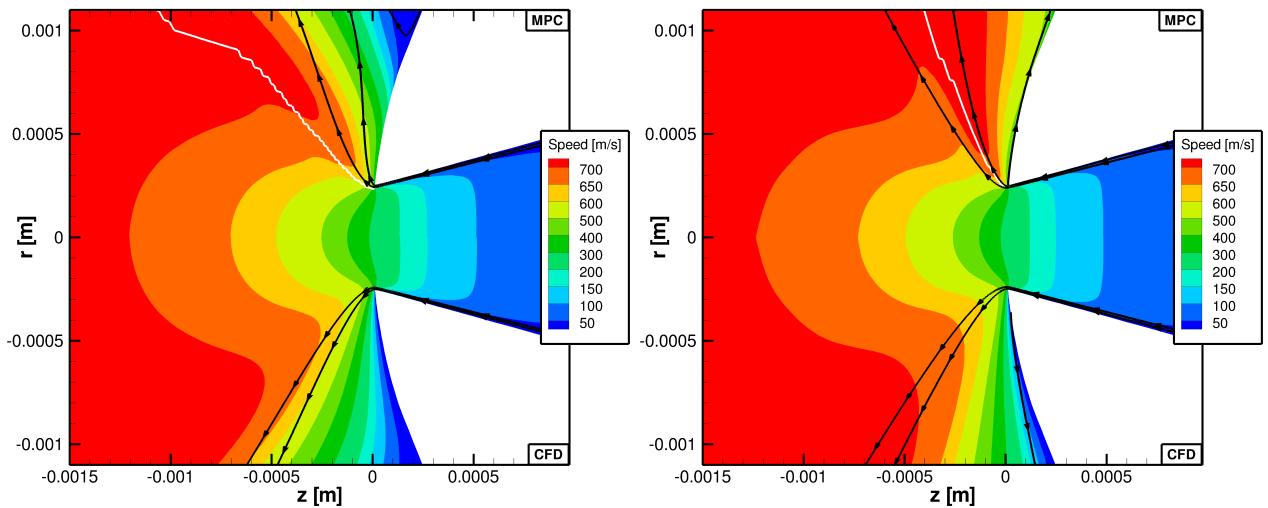
Figures 8(a) and (b) show the pressure contours predicted by the MPC method (top) and full CFD (bottom) at thrust coefficients of  $C_T = 0.5$  and  $C_T = 2.0$ , respectively. Again, the level of disagreement



(a)  $C_T = 0.5$

(b)  $C_T = 2.0$

Figure 6: Comparison of Mach contours and stream lines predicted by continuum (bottom) and hybrid (top) methods around the aeroshell at thrust coefficients of  $C_T = 0.5$  and  $C_T = 2.0$



(a)  $C_T = 0.5$

(b)  $C_T = 2.0$

Figure 7: Comparison of gas speed contours and stream lines predicted by continuum (bottom) and hybrid (top) methods in the jet expansion region at thrust coefficients of  $C_T = 0.5$  and  $C_T = 2.0$



between MPC and CFD predictions in the interaction region increases as the thrust coefficient increases. The agreement of flow quantities within the complex shock layer has a direct effect on the agreement of surface properties which are shown in the proceeding subsection.

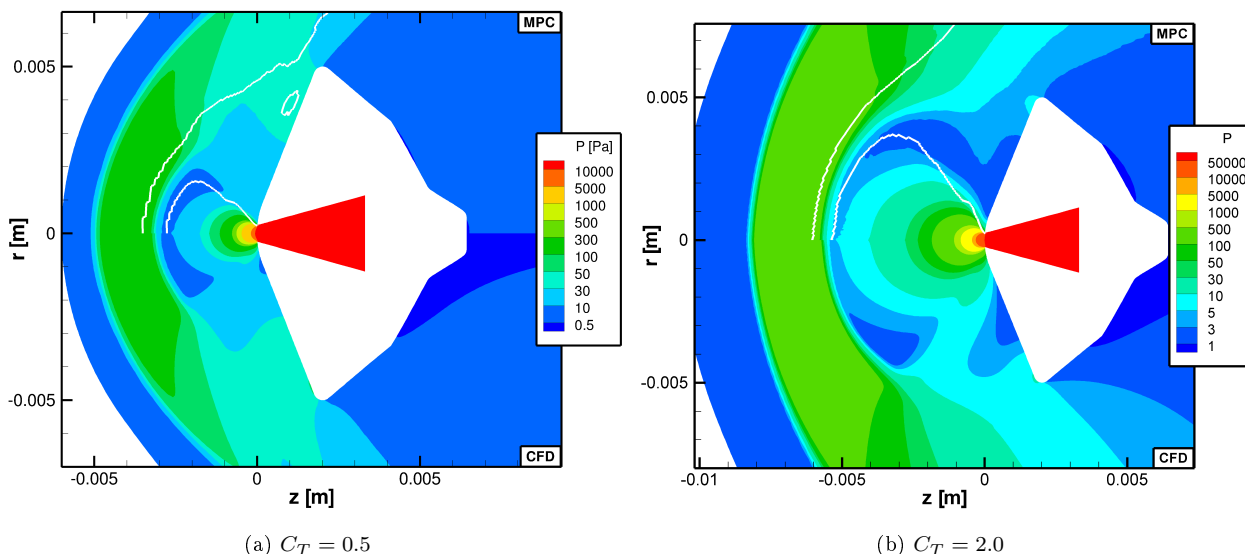


Figure 8: Comparison of pressure contours predicted by continuum (bottom) and hybrid (top) methods around the aeroshell at thrust coefficients of  $C_T = 0.5$  and  $C_T = 2.0$

### Surface Properties

Figure 9(a) shows the surface pressure coefficient, which is defined by Eq. 4, predicted by continuum and hybrid methods along with the surface profile of the maximum gradient-length Knudsen number. Notice that  $Kn_{GL-MAX}$  is greater than 0.05 for nearly the entire surface, indicating the flow is considered in continuum breakdown. Despite the continuum breakdown at the surface, MPC and CFD predictions of the surface pressure are in good agreement along most of the fore-body surface except very near the jet where the MPC method predicts a faster decrease and increase of pressure compared to full CFD. In the wake region, the disagreement increases due to the increase of local Knudsen number and rarefied flow effects. In addition, the change of surface quantities at geometry changes is more diffuse in the continuum predictions compared to the corresponding hybrid predictions.

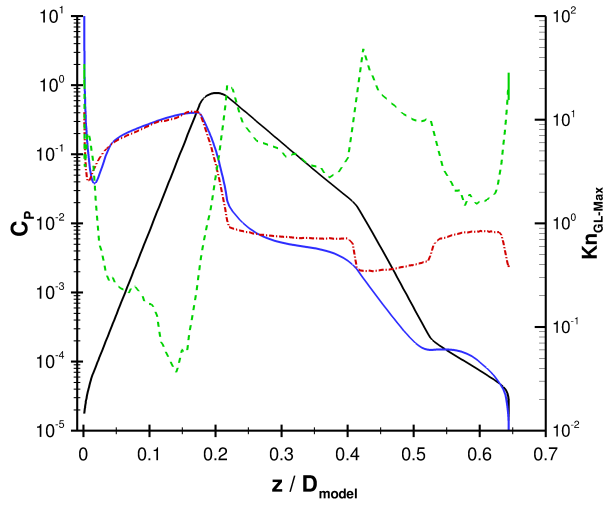
$$C_P = \frac{P}{\frac{1}{2}\rho_\infty U_\infty^2} \quad (4)$$

$$C_\tau = \frac{\tau}{\frac{1}{2}\rho_\infty U_\infty^2} \quad (5)$$

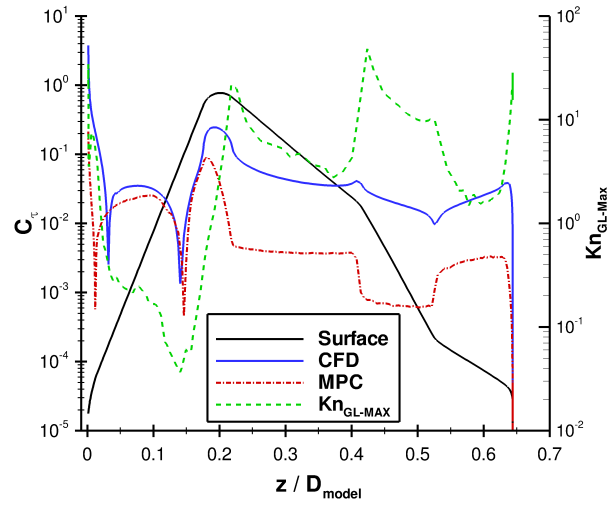
The shear stress coefficient, which is defined by Eq. 5, over the surface of the aeroshell predicted by the MPC method and full CFD is shown in Fig. 9(b). Again, agreement is best in the fore-body and the difference in size of recirculation zone is evident. In the wake region, where rarefied effects become stronger, full CFD over predicts the shear stress by an order of magnitude compared to the MPC prediction. Similar trends are seen in predictions of surface pressure and shear stress at the thrust coefficient of 2.0 which are shown in Figs. 9(c) and (d). However,  $Kn_{GL-MAX}$  is higher along with the level of disagreement between hybrid and continuum predictions along the fore-body. In the wake, the magnitude of  $Kn_{GL-MAX}$  and the level of disagreement between hybrid and continuum predictions remain about the same at each thrust condition.

### Aerodynamic Coefficients

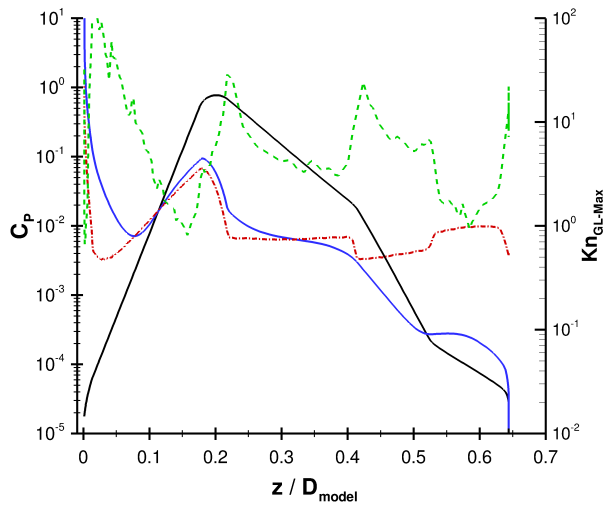
Ultimately, the goal of this study is to assess the effect of rarefied flow on the predictive capability of continuum methods on the aerodynamic coefficients. Figure 10 shows the aerodynamic drag coefficient,



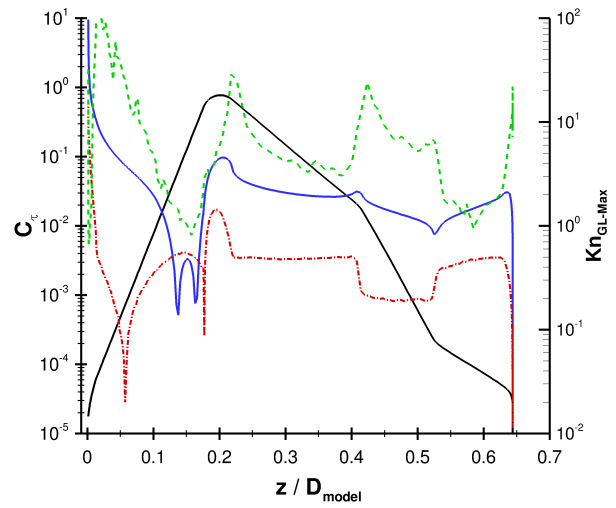
(a) Pressure,  $C_T = 0.5$



(b) Shear,  $C_T = 0.5$



(c) Pressure,  $C_T = 2.0$



(d) Shear,  $C_T = 2.0$

Figure 9: Surface quantities predicted by CFD and the MPC method

calculated using Eq. 6, as a function of thrust coefficient comparing the current hybrid results with previous<sup>12</sup> continuum calculations.

$$C_D = \frac{D}{\frac{1}{2}\rho_\infty U_\infty^2 A} \quad (6)$$

The drag force is calculated by integrating the momentum transfer (through normal pressure and shear stress) to the aeroshell surface. The figure also includes the total axial force coefficient, which is the sum of the aerodynamic drag coefficient and the thrust coefficient, of the aeroshell. Despite the differences in prediction of surface quantities by hybrid and continuum methods, the two methods qualitatively show similar trends with a reduction of the drag coefficient as the thrust coefficient increases. Quantitatively, the continuum method under predicts the drag coefficient predicted by the MPC method by 6% for the low thrust condition. At the high thrust coefficient, full CFD over predicts the drag coefficient of the MPC method by a factor of 2.7. However, because the aerodynamic drag is only a small contribution to the total axial force, continuum and hybrid predictions of the total axial force remain in very good agreement at both thrust conditions. The continuum result under predicts the total aerodynamic force hybrid result by 2.8% at the low thrust condition, while over predicting the hybrid result by 3.9% at the high thrust coefficient.

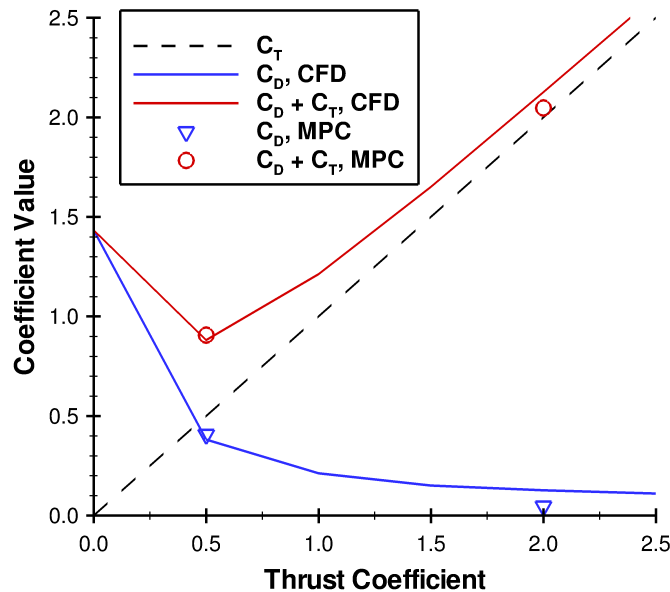


Figure 10: Comparison of aerodynamic coefficients predicted by full CFD and the MPC method

## IV. Conclusion

This study investigated the effects of continuum breakdown on flow field and surface quantities for Mach 12 flow over an aeroshell with an axial, sonic propulsive decelerator jet at two thrust coefficients. Due to the extremely small collision length scales within the jet core, application of a particle method, such as DSMC, to the entire flow is numerically expensive. Instead, a hybrid method is employed that applies the DSMC method only in regions that display rarefied flow effects and employs the continuum description in regions where the Navier-Stokes equations are physically accurate. Qualitatively, both continuum and hybrid predictions of the flow are in agreement for general flow features at both thrust coefficients. However, the continuum results under predict the size of the recirculation zone in the fore-body region compared to the hybrid predictions. In addition, the MPC method predicts a stronger expansion near the jet exit and higher velocity near the vehicle surface. As the thrust coefficient increases, the degree of rarefaction intensifies and level of disagreement between hybrid and continuum predictions broadens. The level of agreement in the flow field has a direct effect on the agreement of surface quantities. Although the level of disagreement in

aerodynamic coefficients increases as the thrust coefficient increases, the total axial force remains in very good agreement at both thrust conditions.

## Acknowledgments

The authors gratefully acknowledge funding from NASA Grants NCC3-989 and NNX08AH37A. The use of supercomputers at the University of Michigan (Center for Advanced Computing) and NASA (NASA Advanced Supercomputing Division) is essential to this work and is also greatly appreciated.

## References

- <sup>1</sup>Zang, T. A. and et al., "Entry, Descent and Landing Systems Analysis Study: Phase 1 Report," *NASA TM-2010-000002009*, May 2010.
- <sup>2</sup>Lofthouse, A. J., Scalabrin, L. C., and Boyd, I. D., "Hypersonic aerothermodynamics analysis across nonequilibrium regimes using continuum and particle methods," AIAA Paper 2007-3903, January, 2007.
- <sup>3</sup>Lofthouse, A. J., Scalabrin, L. C., and Boyd, I. D., "Velocity slip and temperature jump in hypersonic aerothermodynamics," *Journal of Thermophysics and Heat Transfer*, Vol. 22, No. 1, 2008, pp. 38–49.
- <sup>4</sup>Holman, T. D. and Boyd, I. D., "Effects of Continuum Breakdown on the Surface Properties of a Hypersonic Sphere," *Journal of Thermophysics and Heat Transfer*, Vol. 23, No. 4, 2009, pp. 660–673.
- <sup>5</sup>Schwartzentruber, T. E., Scalabrin, L. C., and Boyd, I. D., "A modular particle-continuum numerical method for hypersonic non-equilibrium gas flows," *Journal of Computational Physics*, Vol. 225, No. 1, July 2007, pp. 1159–1174.
- <sup>6</sup>Schwartzentruber, T. E., Scalabrin, L. C., and Boyd, I. D., "Hybrid particle-continuum simulations of nonequilibrium hypersonic blunt-body flowfields," *Journal of Thermophysics and Heat Transfer*, Vol. 22, No. 1, 2008, pp. 29–37.
- <sup>7</sup>Ashkenas, H. and Sherman, F. S., "The Structure and Utilization of Supersonic Free Jets in Low Density Wind Tunnels," *Contract No. NAS7-100, ONR/AFOSR Contract Review*, 1965.
- <sup>8</sup>Codoni, J. R., Reed, E. M., McDaniel, J. C., Alkandry, H., and Boyd, I. D., "Interactions of Peripheral 4-Jet Sonic and Supersonic Retropropulsion Jets on a Mars Science Laboratory Aeroshell," AIAA Paper 2011-1036, January 2011.
- <sup>9</sup>Alkandry, H., Boyd, I. D., Reed, E. M., and McDaniel, J. C., "Numerical Study of Hypersonic Wind Tunnel Experiments for Mars Entry Aeroshells," AIAA Paper 2009-3918, June 2009.
- <sup>10</sup>Alkandry, H., Boyd, I. D., Reed, E. M., Codoni, J. R., and McDaniel, J. C., "Interactions of Single-Nozzle Supersonic Propulsive Deceleration Jets on Mars Entry Aeroshells," AIAA Paper 2011-138, January 2011.
- <sup>11</sup>McGhee, R. J., "Effects of a Retronozzle Located at the Apex of a 140 degree Blunt Cone at Mach Numbers of 3.00, 4.50, and 6.00," *NASA Technical Note D-6002*, January 1971.
- <sup>12</sup>Alkandry, H., Boyd, I. D., Reed, E. M., Codoni, J. R., and McDaniel, J. C., "Interactions of Single-Nozzle Sonic Propulsive Deceleration Jets on Mars Entry Aeroshells," AIAA Paper 2010-4888, June 2010.
- <sup>13</sup>Scalabrin, L. C. and Boyd, I. D., "Development of an Unstructured Navier-Stokes Solver for Hypersonic Nonequilibrium Aerothermodynamics," AIAA Paper 2005-5203, June 2005.
- <sup>14</sup>Scalabrin, L. C. and Boyd, I. D., "Numerical simulation of weakly ionized hypersonic flow for reentry configurations," AIAA Paper 2006-3773, June 2006.
- <sup>15</sup>Scalabrin, L. C. and Boyd, I. D., "Numerical simulations of the FIRE-II convective and radiative heating rates," AIAA Paper 2007-4044, June 2007.
- <sup>16</sup>Bird, G. A., *Molecular Gas Dynamics and the Direct Simulation of Gas Flows*, Clarendon Press, 1994.
- <sup>17</sup>Wang, W.-L. and Boyd, I. D., "Predicting continuum breakdown in hypersonic viscous flows," *Physics of Fluids*, Vol. 15, No. 1, Jan. 2003, pp. 91–100.
- <sup>18</sup>Boyd, I. D., Chen, G., and Candler, G. V., "Predicting failure of the continuum fluid equations in transitional hypersonic flows," *Physics of Fluids*, Vol. 7, No. 1, Jan. 1995, pp. 210–219.
- <sup>19</sup>Holman, T. D., *Numerical Investigation of the Effects of Continuum Breakdown on Hypersonic Vehicle Surface Properties*, Ph.D. thesis, University of Michigan, 2010.
- <sup>20</sup>Deschenes, T. R. and Boyd, I. D., "Application of a Modular Particle-Continuum Method to Partially Rarefied, Hypersonic Flow," *Proceedings of the 27th International Symposium on Rarefied Gas Dynamics*, Asilomar, CA, January 2011.
- <sup>21</sup>Holman, T. D. and Boyd, I. D., "Effects of Continuum Breakdown on the Surface Properties of a Hypersonic Sphere," *Journal of Thermophysics and Heat Transfer*, Vol. 23, No. 4, October-December 2009, pp. 660–673.
- <sup>22</sup>Schwartzentruber, T. E. and Boyd, I. D., "A hybrid particle-continuum method applied to shock waves," *Journal of Computational Physics*, Vol. 215, No. 2, July 2006, pp. 402–416.
- <sup>23</sup>Dietrich, S. and Boyd, I. D., "Scalar and Parallel Optimized Implementation of the Direct Simulation Monte Carlo Method," *Journal of Computational Physics*, Vol. 126, No. 2, July 1996, pp. 328–342.
- <sup>24</sup>Schwartzentruber, T. E., Scalabrin, L. C., and Boyd, I. D., "Multiscale Particle-Continuum Simulations of Low Knudsen Number Hypersonic Flow Over a Planetary Probe," *Journal of Spacecraft and Rockets*, Vol. 45, No. 6, 2008, pp. 1196–1206.
- <sup>25</sup>Deschenes, T. R., Holman, T. D., and Boyd, I. D., "Effects of Rotational Energy Relaxation in a Modular Particle-Continuum Method," *Journal of Thermophysics and Heat Transfer*, Vol. 25, No. 2, 2011, pp. 218–227.
- <sup>26</sup>Dietrich, S., "Scalar and Parallel Optimized Implementation of the Direct Simulation Monte Carlo Method," *Journal of Computational Physics*, Vol. 126, No. 2, July 1996, pp. 328–342.
- <sup>27</sup>Boyd, I. D., "Analysis of rotational nonequilibrium in standing shock waves of nitrogen," *AIAA Journal*, Vol. 28, No. 11, 1990, pp. 1997–1999.

<sup>28</sup>Vijayakumar, P., Sun, Q., and Boyd, I. D., "Vibrational-translational energy exchange models for the direct simulation Monte Carlo method," *Physics of Fluids*, Vol. 11, No. 8, Aug. 1999, pp. 2117-2126.

<sup>29</sup>Sun, Q. and Boyd, I. D., "Evaluation of Macroscopic Properties in the Direct Simulation Method," *Journal of Thermophysics and Heat Transfer*, Vol. 19, No. 3, 2005, pp. 329-335.